



TWIST

Journal homepage: www.twistjournal.net



Novel Metal Complexes of Bioactive Amide Ligands as New Potential Antibreast Cancer Agents

Abdou S. El-Tabl

Faculty of Science, Department of Chemistry, El-Menoufia University, Shebin El-Kom, 13829, Egypt

Moshira M. Abd El-Wahed

Faculty of Medicine, Department of Pathology, El-Menoufia University, Shebin El -Kom, 13829 Egypt

Noha M. El Kadi

Faculty of Medicine, Department of Pathology, El-Menoufia University, Shebin El-Kom, 13829, Egypt

Sherif A. Kolkaila

Faculty of Science, Department of Chemistry, El-Menoufia University, Shebin El-Kom, 13829, Egypt

Mohamed S. Daba*

Faculty of Science, Department of Chemistry, El-Menoufia University, Shebin El -Kom, 13829, Egypt [*Corresponding author]

Abstract

New binary Cu(II), Mn(II), Ag(I), Fe(III), Co(II), Ni(II), Zn(II), Cd(II), Mg(II), Al(III) and Ca(II) metal complexes derived from (Z)-N'-(2-hydroxybenzylidene)-2-((Z)-(2-hydroxybenzylidene)amino)pro p-anehydrazide ligand were prepared. Physicochemical studies (IR, UV - Vis, Mass, 1H-NMR, Magnetism, DTA and TGA, conductivity and ESR) were carried out. The measurements revealed that, the ligand coordinated to the metal ion in a neutral hexadentate or dibasic hexadentate mode through nitrogen atoms of imino group and oxygen atom of the hydroxyl group in protonated or non-protonated form. All metal complexes are non-electrolytic in nature as suggested by molar conductance measurements. The complexes are adopted to be tetragonal distorted octahedral geometry around the metal ions. The cytotoxic activity of the ligand as well as some of its metal complexes was evaluated against breast cancer (MCF-7). It is worth noting, the cytotoxic activity was enhanced upon complexation. Also, it was interestingly found that, Zn(II) complex (7) recorded the highest IC50 value against MCF-7. However, the other tested complexes showed a weak cytotoxicity against the same cell line compared with a standard drug (vinblastine sulfate). The molecular docking of the tested.

Keywords

Amides, Complexes, Spectra, Magnetism, ESR, Cytotoxicity

INDRODUCTION

Complexes was carried out to know the number of bonding and the energy with the breast gene. Amides and their derivatives constitute a amount class of compounds in organic chemistry. These compounds have interesting biological properties such as anti-inflammatory, analgesic, anticonvulsant, antituberculous, antitumor, anti-HIV and antimicrobial activity [1]. Amides are important compounds for drug design, as possible ligands for metal complexes, organocatalysis and also for the syntheses of heterocyclic compounds [2]. The ease of preparation, increased hydrolytic stability relative to imines, and tendency toward crystallinity are all desirable characteristics of amides. Due to these positive traits, amides had been under study for a long time, but much of their basic chemistry remains unexplored. Amides ligands create an environment similar to the one present in biological systems usually by making coordination through oxygen and nitrogen atoms. Various important properties of carbonic acid amides, along with their applications in medicine and analytical chemistry, have led to increased interest in their complexation characteristics with transition metal ions [3]. The

amides unit offers a number of attractive features such as the degree of rigidity, a conjugated system and a NH unit that readily participates in hydrogen bonding and may be a site of protonatione- deprotonation. It is well established that, the formation of metal complexes plays an important role to enhance the biological activity of free hydrazones [4]. Amides ligands are promising compounds because of their ability towards complexation and wide range of biological and nonbiological properties [5]. The chemistry of transition metals with ligands from the amides family has been of interest to coordination as well as bio-inorganic chemists due to their different bonding modes with both electron rich and electronpoor metals. Breast cancer (BC) is the second most common cancer in the world and, by far the most frequent cancer among women. Incidence rates vary nearly fourfold across the world regions, with rates ranging from 27 per 100,000 in Middle Africa and Eastern Asia to 96 in Western Europe [6]. In USA about 19% of breast cancers are diagnosed in women ages 30e49 years, and 44% occur among women who are age 65 years or older [7]. In most African countries, BC among young women comprises a high proportion of cases than among older women. This is a demography driven phenomenon rather than a true intrinsic biologic significance, because the African population has a low median age; generally 20 years and below [8]. The median age at diagnosis in Arab populations, is about 48 years, and about two-third of women with BC are younger than 50 years [9]. In Egypt the incidence rate of breast cancer is 29.9/100,000 population in the age group of 30-34 years. In a study comparing Egypt's Gharbia Cancer Registry (GCR) and the United States Surveillance, Epidemiology, and End results (SEER) registries, Egyptian GCR cases were, on average, over 10 years younger than US SEER cases, with nearly 19% of GCR cases 40 years of age as compared to only 6% of US SEER cases [10]. Continue to our work, new metal complexes of new amid ligand derived from 4-amino salicylic acid have been prepared and spectroscopically characterized and also the cytotoxic activity of the ligand and its metal complexes were studied against MCF-7 cell line and also molecular docking program was carried out.

MATERIALS AND METHODS

The ligand and its metal complexes were analyzed for C, H, N, Cl and M at the Micro Analytical Center, Cairo University, Egypt. Standard analytical methods were used to determine the metal ion content [11]. ¹H-NMR spectra were obtained on bruker 400 MHz spectrometer. Chemical shifts (ppm) are reported relative to TMS. FT-IR spectra of the ligand and its metal complexes were measured using KBr discs by a Jasco FT/IR 300E Fourier transform infrared spectrophotometer covering the range 4000-400 cm⁻¹. The mass spectra of the compounds were recorded on JEOL JMS-XA- 500 mass spectrometer. Electronic spectra in the 200-900 nm regions was recorded on a Perkin-Elmer 550 spectrophotometer. The thermal analyses (DTA and TGA) were carried out on a Shimadzu DT-30 thermal analyzer from room temperature to 800 °C at a heating rate of 10 °C/min. Magnetic susceptibilities were measured at 25°C by the Gouy method using mercuric tetrathiocyanatocobaltate(II) as the magnetic susceptibility standard. Diamagnetic corrections were estimated from Pascal's constant 30. The magnetic moments were calculated from the equation:

$$(\mu \text{ eff} = 2.828 (Xn \times T)^{-1/2})(1)$$

The molar conductance of 10⁻³ M solution of the complexes in DMSO was measured at 25°C with a Bib by conductometer type MCl. The ESR spectra of solid complexes at room temperature were recorded using a varian E-109 spectrophotometer; DPPH was used as a standard material. The TLC of all compounds confirmed their purity.

Synthesis of the ligand

The ligand, ($\mathbf{H_4L}$) was synthesized by boiling (10.0 g, 1.4 mol) of 4-amino salicylic acid in 50 cm³ of ethanol solution in the presence of 5 drops of Conc $\mathbf{H_2SO_4}$ for two hours. Leave it to cool at room temperature to give 4-amino salicylic ester that was mixed with(8.0g,0.4mol) ortho phenylenediamine. The solution was refluxed with stirring for two hours at 80 °C, then left to cool at room temperature. The precipitated product was filtered off then dried under vacuum over anhydrous CaCl₂. (5.0 g, 0.12 mol) of the yield reacted with (3.0 g, 0.04 mol) of salcylaldhyde in the presence of 50 cm³ of ethanol solution. The solution was refluxed for another two hours with stirring at 80 °C, then left to cool at room temperature. The precipitate was filtered off, and then dried under vacuum to give the ligand, (Figure 1).

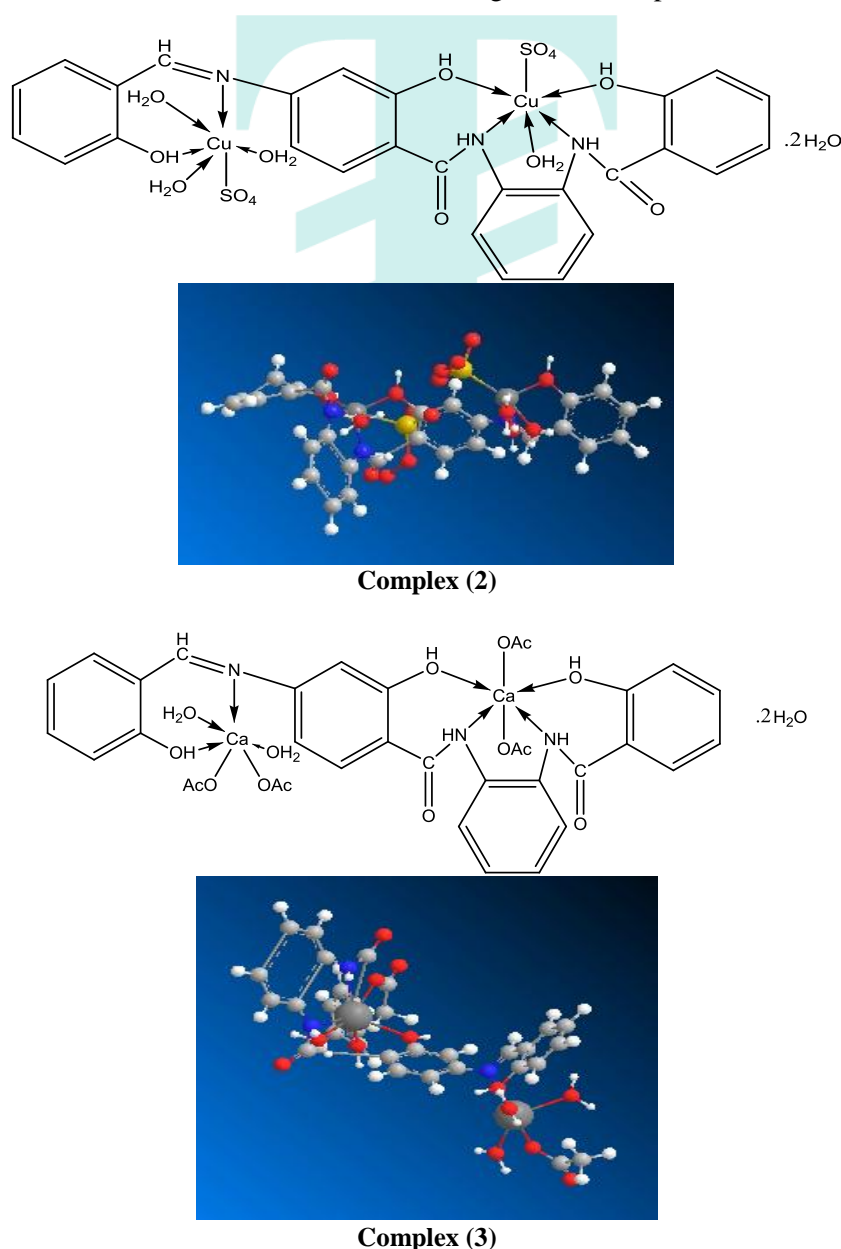
$$\begin{array}{c|c} & & & \\ & & & \\ & & & \\ & & & \\ & & & \\ & & & \\ & & & \\ & & & \\ & & & \\ & & & \\ & & & \\ & & & \\ & & & \\ & & & \\ & & \\ & & & \\ & &$$



Figure 1 Chemical and 3D Structures of the ligand [H₄L] (1)

PREPARATION OF METAL COMPLEXES

Complexes was synthesized using (1L:2M) molar ratio, by refluxing of (1.0 g, 0.04 mol) of the ligand dissolved in 30 cm³ ethanol with 30 cm³ ethanolic solution of the metal salts, (0.65g, 0.02 mol) CuSO₄.5H₂O complex(**2**), (0.63g, 0.02 mol) Ca (OAc)₂.2H₂O complex (**3**), (0.78g, 0.02 mol) ZnSO4.2H₂O complex (**4**), (0.94g, 0.02 mol) CoSO₄.7H₂O complex (**5**), (0.86g, 0.02 mol) Mn(CO3)₂.4H₂O complex (**6**), (0.69g, 0.02 mol)[NiSO4.4H₂O] complex (**7**), (0.66g, 0.02 mol) Cd(OAc)₂.5H₂O complex (**8**), (0.82g, 0.02 mol) FeSO4.4H₂O complex (**9**), (0.49g, 0.02 mol) Al₂(SO₄)₃.4H₂O complex (**10**), (0.98g, 0.02 mol) AgNO₃.3H₂O complex (**11**), for two hours under continuous stirring at 80 °C. The obtained precipitate were filtered off and dried in desiccators over CaCl₂ to give new complexes.

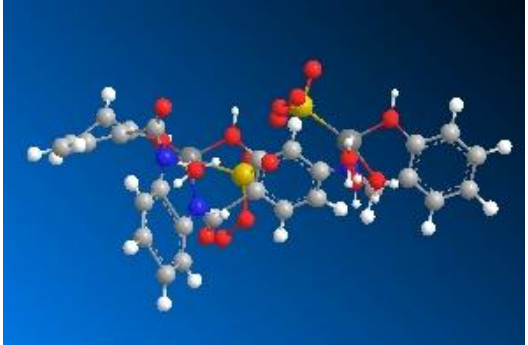


$$\begin{array}{c|c} H \\ C \\ N \\ OH \\ SO_4 \end{array}$$



Complex (4)

$$\begin{array}{c|c} H \\ C \\ N \\ OH \\ CO \\ OH_2 \\$$

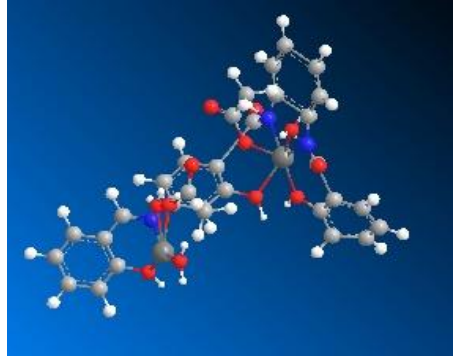


Complex (5)

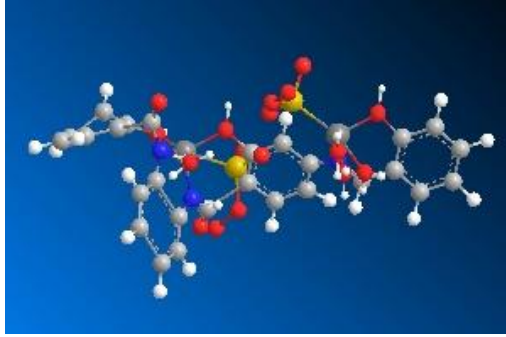
$$\begin{array}{c|c} H \\ C \\ N \\ OH \\ OH_2 \\ OH_2$$



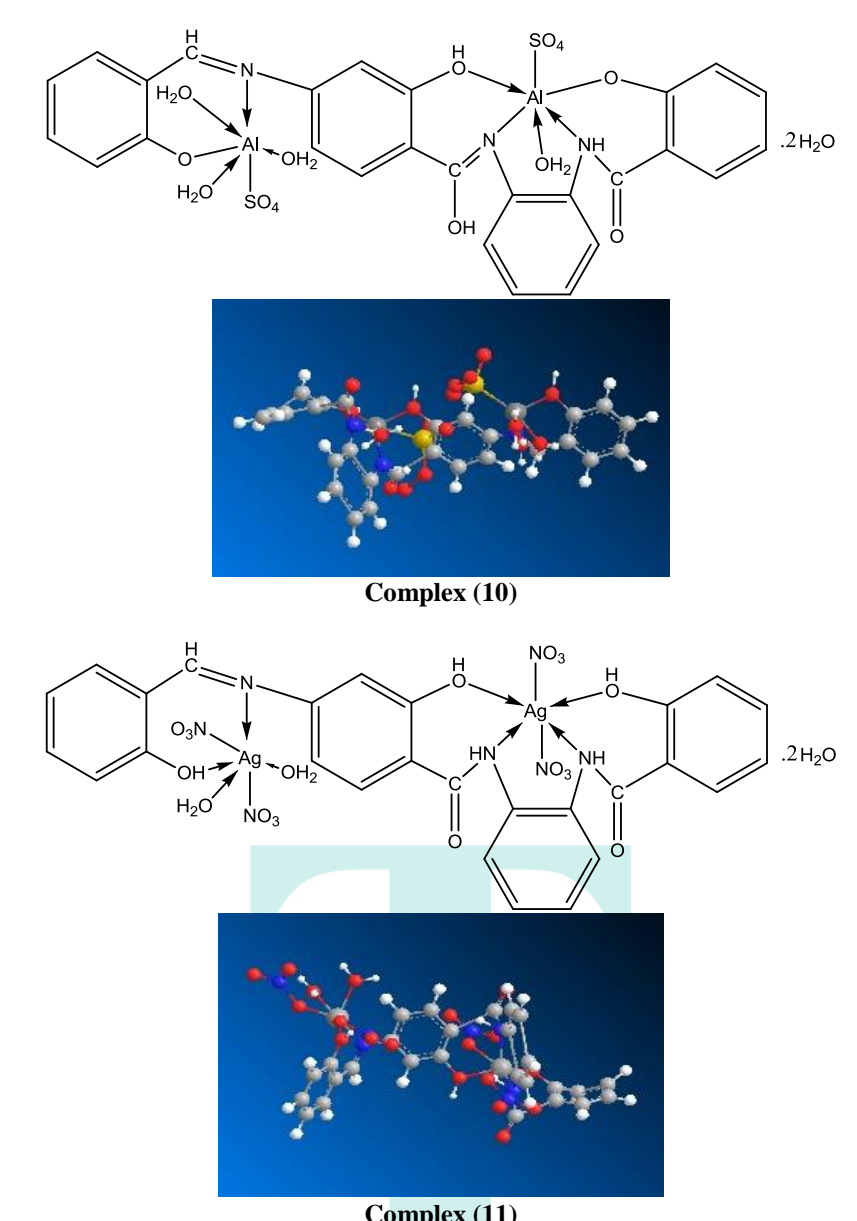
Complex (6)



Complex (8)



Complex (9)



Complex (11)

Figure 2 Chemical and 3D structures of the prepared metal complexes

Table 1 Analytical and Physical Data of the Ligand [H₄L] and its Metal Complexes

No	Ligands/Complexes	Color	FW	МР	Yield (%)	An	Molar conductance *			
						C	H	N	M	
1	$[H4L] C_{27}H_{19}N_3O_4$	Off white	449	350	91	65.68 (64.90)	5.50 (5.30)	13.50 (13.45)	_	-
2	[(H4L)(Cu)2 SO4)2 (H2O)2]. C ₂₇ H ₂₇ N ₃ O ₁₆ S ₂ Cu ₂	black	771	>300	82	41.4 (40.9)	4.58 (4.21)	5.78 (5.55)	17.49 (17.10)	9.56
3	[(H4L)(Ca)2(CH3COO)4(H2O)2]. C ₃₅ H ₃₅ N ₃ O ₁₄ Ca ₂	Dark green	761	>300	86	42.33 (41.8)	4.96 (4.4)	5.92 (5.10)	15.49 (14.10)	8.6
4	[(H4L)(Zn)2(SO4)2(H2O)2]. C ₂₅ H ₃₅ N ₃ O ₁₄ Ni ₂	Pale Yellow	773	>300	85	41.88 (41.00)	5.89 (4.25)	11.46 (9.50)	16.37 (14.30)	10
5	[(H4L)(Co)2(SO4)2(H2O)4]. C ₂₇ H ₂₇ N ₃ O ₁₆ S ₂ Co ₂	Dark Orange	767	>300	79	41.12 (40.12)	4.55 (4.30)	5.75 (9.54)	17.9 (15.12)	9.6
6	[(H4L)(Mn)2(CO3)4(H2O)2]. C ₃₁ H ₂₃ N ₃ O ₁₈ Mn ₂	Brown	725	>300	80	46. 33 (45.23)	5.13 (4.52)	6.48 (9.85)	7.50 (6.14)	10.2
7	[(H4L)(Ni)2(SO4)2(H2O)4]. C ₂₇ H ₂₇ N ₃ O ₁₆ S ₂ Ni ₂	Pale green	769	>300	85	40.22 (40.12)	4.09 (4.15)	8.53 (8.65)	22.81 (23)	9.2
8	[(H4L)(Cd)2(CH3COO)4(H2O)4]. C ₃₅ H ₃₅ N ₃ O ₁₄ Cd ₂	Dark Off white	817	>300	80	28.41 (28.13)	3.51 (3.0)	5.85 (8.16)	17.69 (13.52)	8.5
9	[(H4L)(Fe)2(SO4)2(H2O)4]. C ₂₇ H ₂₇ N ₃ O ₁₆ S ₂ Fe ₂	Greenish Blue	765	>300	83	28.8 (25.12)	3.5 (3.12)	5.9 (8.23)	16.56 (11.56)	6.35
10	[(H4L)(Al)2(SO4)2(H2O)4]. C ₂₇ H ₂₇ N ₃ O ₁₆ S ₂ Al ₂	White	739	>300	85	28.78 (25.32)	3.55 (2.95)	5.92 (8.63)	16.62 (11.12)	8.4
11	[(H4L)(Ag)2(NO3)4(H2O)4]. C ₂₇ H ₂₃ N ₇ O ₁₈ Ag ₂	yellow	827	>300	82	23.52 (24.01)	3.13 (3.54)	4.84 (4.96)	31.64 (32.15)	7.4

RESULT AND DISCUSSION

The ligand and its metal complexes are non-hydroscopic, colored, crystalline and air-stable at room temperature for a long period. They are soluble in dimethylformamide (DMF) and dimethylsulfoxide (DMSO) but insoluble in water, ethanol, methanol, benzene, toluene, acetonitrile and chloroform. The analytical and physical data Table (1) and spectral data (Tables (2) and (3)) are consistent well with the proposed structures Figure 2. Many attempts were carried out to prepare a single crystal but unfortunately they were failed until now. The analytical data indicated that, all complexes formed in 1L: 2M molar ratio.

Conductance measurements

1x10⁻³ molar solutions of the ligand and its metal complexes in DMSO were used for molar conductivities measurements. The compounds recorded low molar conductivities values Table 1 referring that, both the ligand and its metal complexes have non-electrolytic nature [12-13], which confirmed coordination of the anions to the metal ions.

Mass spectra

Mass spectrum of the ligand showed a molecular ion peak at m/e 311amu, corresponding to its formula weight (F.W.311) and supporting the, proposed structure and the purity of the ligand prepared. The prominent mass fragmentation peaks observed at m/z = 55, 65, 93, 121, 223, 240, 311 amu are corresponding to C_4H_7 , C_5H_5 , C_7H_9 , C_9H_{13} , $C_{15}H_{13}$ NO , $C_{15}H_{14}$ NO₂ , $C_{17}H_{17}N_3O_3$ moieties respectively and also support the suggested structure of the ligand. While mass spectrum of the Zn(II) complex (4) showed a molecular ion peak at m/e 730 amu corresponding to its formula weight (F.W. 730) and supporting the proposed structure, and the purity of the complex prepared. The prominent mass fragmentation peaks observed at m/z = 55,93 223, 240, 515, 559, 730 amu are corresponding to C_4H_7 , C_7H_9 , $C_{17}H_{19}$, $C_{17}H_{22}N$, $C_{22}H_{30}ZnN_2O_8$, $C_{23}H_{32}ZnN_3O_9$, $C_{25}H_{35}$ Zn₂N₃O₁₄ moieties respectively and also support the suggested structure of the this complex.

IR spectra of the ligand [H₄L](1) and its metal complexes

The IR spectral data of the ligand and its metal complexes are represented in Table (2). The spectrum of the ligand showed broad bands centered at 3450 and 3373 cm⁻¹ which assigned to $\nu(OH)$. However, strong broad bands appeared in the 3600-3320 and 3380-2670 cm⁻¹ ranges confirmed the presence of non-equivalent intra and intermolecular hydrogen bondings [14-18]. Also, the spectrum of the ligand displayed tow bands at 1700 and 1650cm⁻¹ assignable to $\nu(C=O)$ and $\nu(C=N)$ respectively [19-22]. Medium bands were observed at 1540, 1450, 818 and 750 cm⁻¹ which are related to vibration of $\nu(Ar)$ ring. The $\nu(NH)$ of the ligand appeared at 3190 cm⁻¹, however, The mode of bonding of the ligand can be predicted by comparing the IR spectra of the complexes with that of the free ligand. The complexes showed a broad band in the 3570-3100 cm⁻¹ range, assigned to the presence of hydrated or coordinated water molecules and the bands appeared in the 3650-2610 cm⁻¹ range was due to intra-and intermolecular hydrogen bondings. The $\nu(NH)$ group appeared in the 3190 -3142 cm⁻¹ ranges. The complexes showed $\nu(C=O)$ and $\nu(C=N)$ at 1682-1610 and 1675-1570 cm⁻¹ ranges respectively. These bands were shifted to lower frequency suggesting the participation of the carbonyl and azomethine groups in the coordination process.

Table 2 IR frequencies of the bands (cm⁻¹) of ligand [H4L] (1) and its metal complexes and their assignments.

No.	v(H ₂ O)	v(OH)	υ(H-bonding)	v(NH)	v(C=O)	v(C=N)	v(Ar)	v(OAc)/SO ₄		υ(M-N)
1	3370-3220	3450,3373	3600-3320, 3380-2670	3190	1700	1650	1540,1450,818 ,750	-	-	-
2	3370-3130	3420, 3375	3650-3280, 3270-2650	3155	1615	1610	1486,1430,850 ,765	1430,1340	615	525
3	3560-3370 3320-3180	3420,3379	3600-3210 3200-2700	3150	1610	1635	1486,1430, 850,765	1260,1125 1190,735	610	516
4	3325-3160	3415	3550-3340, 3340-2650	3150	1681	1664	1540,1510, 850,768	1430,1360	618	580
5	3325,3100	3422,	3650-3330, 3320-2675	3178	1610	1615	1540,1515, 850,768	1465,1340	630	537
6	3300,3150	3415	3640-3325, 3320-2870	3160	1682	1650	1486,1430,850 ,765	-	610	520
7	3510-3350 3315,3170	3418, 3245	3610-3330, 3310-2870	3180	1614	1612	1470,1438, 852,753	1354,1461	610	530
8	3350-3185	3400, 3385	3645-3260 3210-3260	3187	1680	1605	1470,1438, 852,753	1260,1260 1093,690	640	520
9	3320-3165	3420	3650-3350, 3340-2670	3170	1655	1670	1540,1515, 850,768	1470,1355	618	560
10	3325-3160	3415	3550-3340, 3340-2650	3150	1681	1664	1540,1510, 850,768	1430,1360	618	580
11	3320-3165	3420	3650-3350, 3340-2670	3170	1655	1670	1540,1515, 850,768	1470,1355	618	560

Electronic spectra

The electronic absorption data of the ligand and its metal complexes in dimethylformamide (DMF) are given in Table (3). The ligand [H4L] showed three bands at 285, 320 and 355 nm are due to $\pi \rightarrow \pi^*$ transitions within the aromatic moieties, $n\rightarrow\pi^*$ transition of chromophore moieties present in the ligand, and CT transitions, respectively [26,30] The electronic absorption spectra of Cu(II) complexes (2), and (3) showed bands at 260, 300, 318, 440, 560 and 610 nm and 275, 320, 455, 510 and 620 nm and 265,305, 318, 435, 570 and 630 nm and respectively, the first bands are due to intraligand transitions however, the other bands correspond to ${}^2B_{1g}(d_{x2-y2)} {\longrightarrow} {}^2A_{1g}d_{z2}$ (v1) $2B1g(dx2-y2) {\longrightarrow} 2B2g(dxy)$ (v2) and 2B1g(dx2-y2)→2Eg(dzy,dxz) (v3) transitions. The position as well as the broadness of these bands suggest that these complexes have a tetragonal distorted octahedral geometry [31,33] This could be due to the Jahn teller effect that operates on the d⁹ electronic ground state of six coordinate system, elongating one trans pair of coordinate bonds and shortening the remaining four ones [34,35]. Magnetic moment values are in the range (1.65-1.75) B.M. corresponding to one unpaired electron, spin-only value. The electronic absorption spectra of Ni(II) complexe (7) displayed bands at 280, 330,420, 460, 540, 600 and 750 nm attributable to intra-ligand transitions and the other bands are assigned to ${}^{3}A_{2g}(F) \rightarrow {}^{3}T_{2g}(F)(v_1)$, ${}^{3}A_{2g}(F) \rightarrow {}^{3}T_{1g}(v_2)$ and ${}^{3}A_{2g}(F) \rightarrow {}^{3}T_{1g}(P)(v_3)$ transitions respectively, which are consistent with octahedral geometry [36,37] This observation is further confirmed by μ_{eff} value (3.06 B.M) corresponding to two unpaired electrons [38]. The v_2/v_1 ratio is 0.95 which are less than the usual range of octahedral nickel(II) complex, indicating that, the nickel(II) complexes have distorted octahedral geometry [39-40]. Mn(II) complex (6) shows bands at 270, 300, 370, 420, 495, 590, and 615 nm, corresponding to intra-ligand transition. Co(II) complex (5) show bands at 275, 300, 385, 420, 585, and 615 nm are due to intra-ligand transitions and indicating octahedral structure which confirmed by $M_{eff} = 4.52$. However, Fe(III) complexe (9) gave bands at 265, 303, 315, 465, 530, and 630 and 270, 300, 320, 460, 570 and 630 nm corresponding to intra-ligand transition and indicating octahedral structure which confirmed by $M_{eff} = 2.72$ and 6.03 B.M respectively. The bands observed for the diamagnetic: complexes (4), (8), and (10) are due to intra-ligand transitions table 3.

Table 3 The electronic absorption spectral bands (nm) and magnetic moments B.M.) for the ligand and its complexes.

Comp. No.	λ_{\max} (nm)	μeff.
1	285, 320, 355	-
2	260, 300, 318, 440, 560, 610	1.65
3	270, 300, 370, 420, 495, 590, 615	5.72
4	275, 310, 320, 445, 565, 625, 710	Diamagnetic
5	255, 300, 320	2.91
6	260, 300, 315,	3.51
7	275, 300, 385, 420, 585, 615	4.52
8	275, 320, 455, 510, 620	Diamagnetic
9	280, 330, 420, 460, 540, 600,750	3.06
10	275, 300, 310, 445, 575, 645	Diamagnetic
11	265, 310, 315	4.72

THERMAL ANALYSES

The thermal data of complexes (2), (6), (7) and (8) are listed in Table (4). These complexes were introduced as representative examples. the thermogram of complex (2) [(H₄L)(Cu)₂(SO₄)₂(H₂O)₄] involving breaking of H-bondings accompanied with endothermic peak at 45 °C. In the second step, three molecules of hydrated water were lost endothermically with peak at 80 °C. accompanied by 9.1 % (Calc 9.2%) weight loss. Loss of coordinated water molecules was recorded in the third step as an endothermic peak observed at 150 °C with 3.3 (Calc. 3.4) weight loss. The 18.6 % weight loss (Calc 18.6%) accompanied by an endothermic peak appears at 245 °C was assigned to loss of sulphat(SO₄), whereas the exoothermic peak observed at 325°C refers to the melting point of the complex. The final step observed in 350,380, 450,500 and 590°C with 17.6 % weight loss (Calc 17.6%), refers to complete oxidative decomposition of the complex which exoed up with the formation of CuOThe first step observed in the thermogram of complex (6) [(H₄L)(Mn)₂CO₃)₄(H₂O)₂] involves breaking of H-bondings accompanied with endothermic peak at 45 °C. In the second step, three molecules of hydrated water were lost endothermically with a peak at 85 °C accompanied by 10.4% (Calc 10.5%) weight loss. The third step involved weight loss 25.5% (Calc 25.6%) weight loss accompanied by an endothermic peak was observed at 160 °C, which was ascribed to loss of a coordinated two two acetat groups (OAc), while the exothermic peak appeared at 355°C refers to the melting point of the complex. The final step observed at 405, 450, 485, 565 and 580 °C with 21.5 % weight loss (Calc 21.5 %) exothermic peaks, refers to complete oxidative decomposition of the complex which ended up with the formation of NiO. The first step observed in while The first step observed in the thermogram of complex (7) [(H₄L)(Ni)₂(SO₄)₂(H₂O)₄] involves breaking of H-bondings accompanied with endothermic peak at 45 °C. In the second step, two molecules of hydrated water were lost endothermically with a peak at 80 °C

accompanied by 7.8% (Calc 7.9%) weight loss. Loss of coordinated water molecules was recorded in the third step as an endothermic peak observed at 130 °C with 4.2 (Calc. 4.3) weight loss. The 14.8 % weight loss (Calc 14.9%) accompanied by an endothermic peak appears at 240 °C was assigned to loss of sulphat(SO₄), whereas the exoothermic peak observed at 350°C refers to the melting point of the complex. The final step observed in 400, 450, 490, 560 and 590°C with 21.4 % weight loss (Calc 21.6%), refers to complete oxidative decomposition of the complex which exoed up with the formation of NiO.Thermogram of complex (8) [(H₄L)(Cd)2(CH3COO)4(H2O)2] showed a decomposition in five steps, the first step involving breaking of H-bondings accompanied with endothermic peak at 50 oC. In the second step, three molecules of hydrated water were lost endothermically with peak at 80 oC accompanied by 10.36 % (Calc 10.4%) weight loss. Such a low temperature endothermic dehydrations indicated that the water molecules were not coordinated to the metal. The 24.32% weight loss (Calc 24.39%) accompanied by an endothermic peak which observed at 170 oC was assigned to loss of two acetat groups (OAc), whereas the exothermic peak observed at 315 oC refers to the melting point of the complex. The final step observed as exothermic peaks 450, 500, 550, 570 and 590 oC with 32.1% weight loss (Calc 32.3%), refers to complete oxidative decomposition of the complex which exoed up with the formation of NiO.

Table 4 Thermal analyses for some metal (II) complexes

Table 4 Thermal analyses for some metal (II) complexes											
Compound No.	Temp. (°C)		DTA (peak) TGA (Wt. loss %)			— Assignments					
Compound 140.	<u> </u>	Endo	Exo	Calc.	Found						
	45	Endo	-	-	-	Broken of H-bondings					
	80	Endo	-	9.18	9.21	Loss of(3H ₂ O) hydrated water molecules					
	150	Endo	-	3.37	3.42	Loss of (H ₂ O)Coordinate water molecules					
Complex (2)	245	endo	-	18.6	18.69	Loss of(SO ₄)					
	325	Exo	-	-	-	Melting point					
	350,380,450, 500,590	-	Exo	17.61	17.67	Decomposition process with the formation of CuO					
	45	Endo	-	-	-	Broken of H-bondings					
	85	Endo	-	10.48	10.5	Loss of (3H ₂ O) hydrated water molecules					
	160	Endo	-	25.59	25.6	Loss of 2(OAC) group					
Complex (6)	355	-	Exo	-	-	Melting point					
	405,450,485, 565,580	-	Exo	21.57	21.59	Decomposition process with the formation of NiO					
	45	Endo	-	-	-	Broken of H-bondings					
	140	Endo	-	7.8	7.9	Loss of (2H ₂ O) hydrated water molecules					
	130	Endo	-	4.25	4.33	Loss of (H ₂ O) Coordinated water molecules					
G 1 (7)	240,260	Endo	_	1481	14.9	Loss of SO ₄ group					
Complex (7)	350	_	Exo	_	-	Melting point					
	400,450,490, 560,590		Exo	21.44	21.66	Decomposition process with the formation of NiO					
	50	Endo	-	-	-	Broken of H-bondings					
	80	Endo	-	7.17	7.21	Loss of (2H ₂ O) hydrated water molecules					
Complex (9)	230	Endo	-	24.38	`24.41	Loss of (SO ₄)group					
Complex (9)	425	-	Exo	-	-	Melting point					
	420,500,550, 610	-	Exo	21.58	21.61	Decomposition process with the formation of FeO					
	50	Endo	-	-	-	Broken of H-bondings					
	80	Endo	-	6.26	6.32	Loss of (2H ₂ O) hydrated water molecules					
	150	Endo	-	3.33	3.49	Loss of (H ₂ O) coordinated water molecules					
Complex (11)	220	Endo		18.4	`18.47	Loss of (CO ₃) group					
	420	_	Exo	_	-	Melting point					
	390,450,500, 550,600	-	Exo	18.58	19.1	Decomposition process with the formation of CuO					

Docking test

In the present study the selected protein 3s7s represents the crystal structure of the human placentalany proposed biologically active compound. This approach elucidates the ligand-receptor site and type of interactions. It also gives an estimation of the distance between the ligand and the receptor inside the interaction grid. The scoring energy of each pose simulated by the docking calculations reflects the degree of inhibition effect of the correspondingligand. In the present

study, the selected protein 3s7s represents the crystal structure of the human placental aromatase enzyme that catalyzes the synthesis of estrogen hormone and contributes to estrogen-dependent breast cancer50. All ligands possess an appreciable extent of interactions with the receptor protein based on the scoring energy. The result shows the ability of ligand to inhibit 3s7s protein.

Ligand

The docked (ligand) Fig. 1 have effective ligand-receptor interaction distances were ≤ 3.5 A in most cases, which indicates the presence of typical real bonds and hence high binding affinity. For example, the nearest interaction is observed via H-donors with 3S7S (3.01A) and (ligand) With Moledock score (S) 34196 Furthermore, fourteen binding sites were observed of different amino acids (Gln 225, His 480, Asp 222, Arg192, Gln 218, pro 308, Asp 309 and lle 474) with ligand demonstrating their high inhibition.

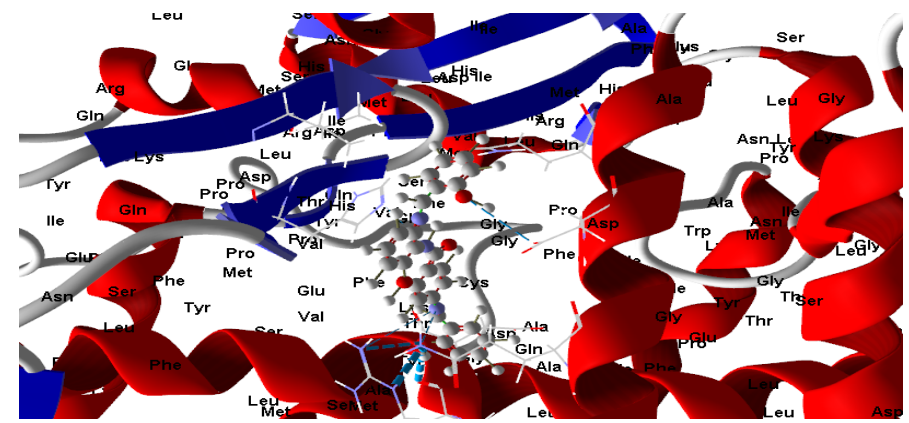


Figure (1) Virtual Molecular docking of the best docked (ligand) with 3s7sprotein

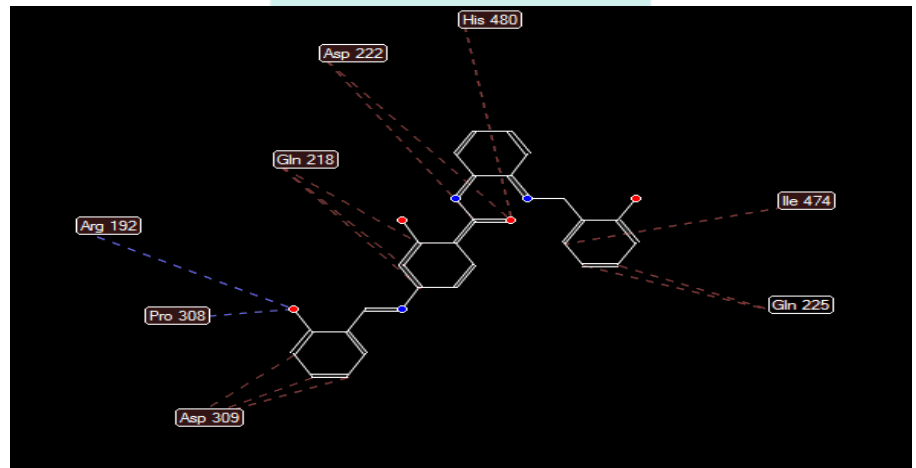


Figure (2) 2D structure of Molecular docking of (ligand) with 3s7sprotein

Complex 1

While the docked (complex 1) Fig. 3 have effective ligand-receptor interaction distances were \leq 3.5 A in most cases, which indicates the presence of typical real bonds and hence high binding affinity. For example, the nearest interaction is observed via H-donors with 3S7S (2.14A) and (complex 1) With moldock score113829 Furthermore, twenty-one binding sites were observed of different amino acids(His480 ,Phe 221,Gln 218, Asp 222, Gln 225 and Arg 192) with complex 1 demonstrating their high inhibition.

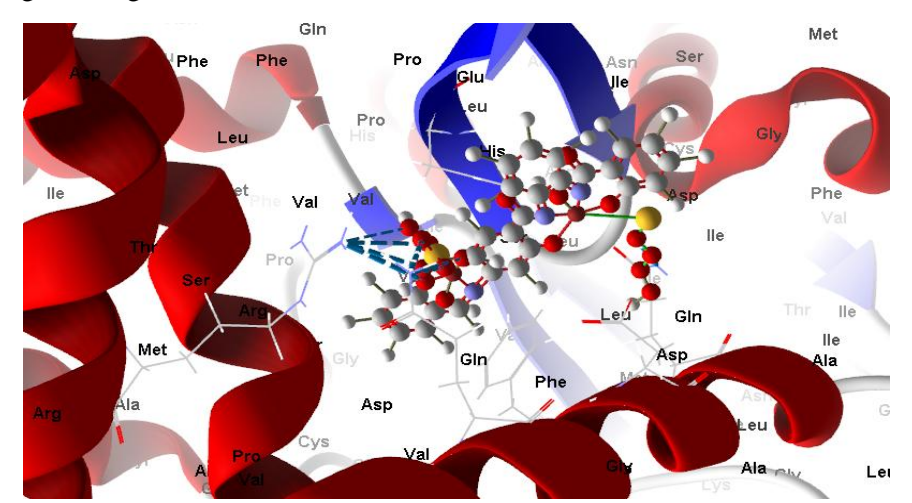


Figure 3 Virtual Molecular docking of the best docked (complex 1) with 3s7sprotein

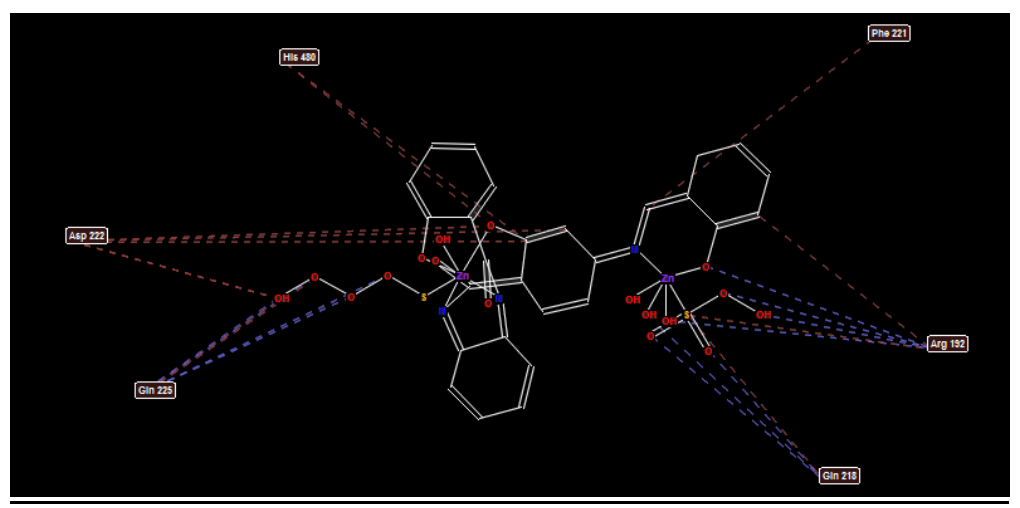


Figure 4 2D structure of Molecular docking of (complex 1) with 3s7sprotein

Complex 2

However, the docked (complex 2) Fig. 5 have effective ligand-receptor interaction distances were \leq 3.5 A in most cases, which indicates the presence of typical real bonds and hence high binding affinity . For example, the nearest interaction is observed via H-donors with 3S7S (2,71A) and (complex 2) With Moldock score203137 Furthermore, twenty seven binding sites were observed of different amino acids (Gln 218, Arg 192, Glu483,His 480,Asp222, Asp 309, Asp 482, Pro 309, Val 313 and Phe 221) with complex 2representing the excellent inhibition.

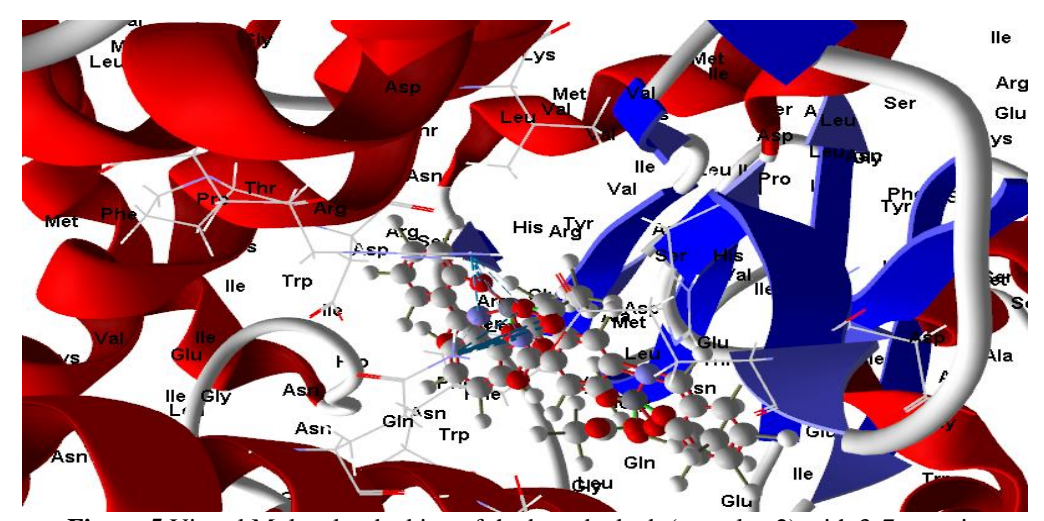


Figure 5 Virtual Molecular docking of the best docked (complex 2) with 3s7sprotein

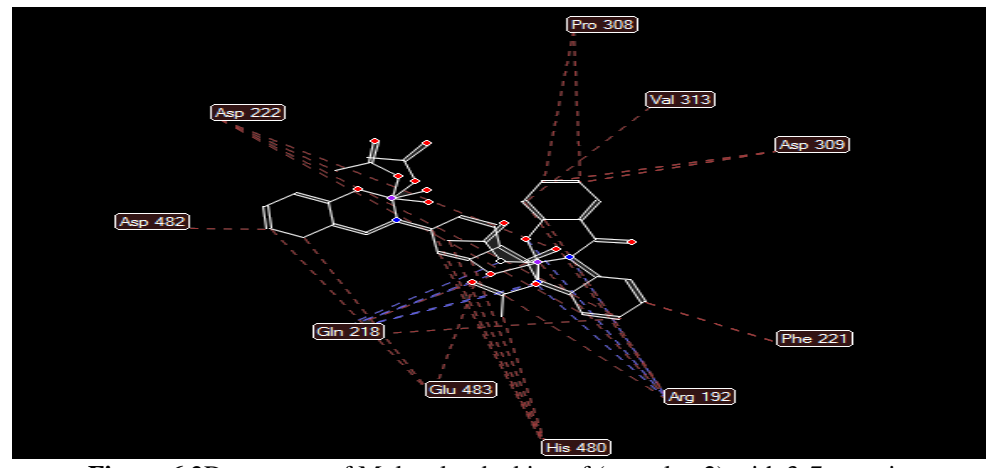


Figure 6 2D structure of Molecular docking of (complex 2) with 3s7sprotein

Complex 3

While the docked (complex 3) Fig. 7 have effective ligand-receptor interaction distances were \leq 3.5 A in most cases, which indicates the presence of typical real bonds and hence high binding affinity. For example, the nearest interaction is observed via H-donors with 3S7S (2.34A) and (complex 3) With moldock score 125957 Furthermore, nineteen binding sites were observed of different amino acids(His480 ,Phe 221,Gln 218, Asp 222, Gln 225, Glu 483 and Arg 192) with complex 3 demonstrating their high inhibition.

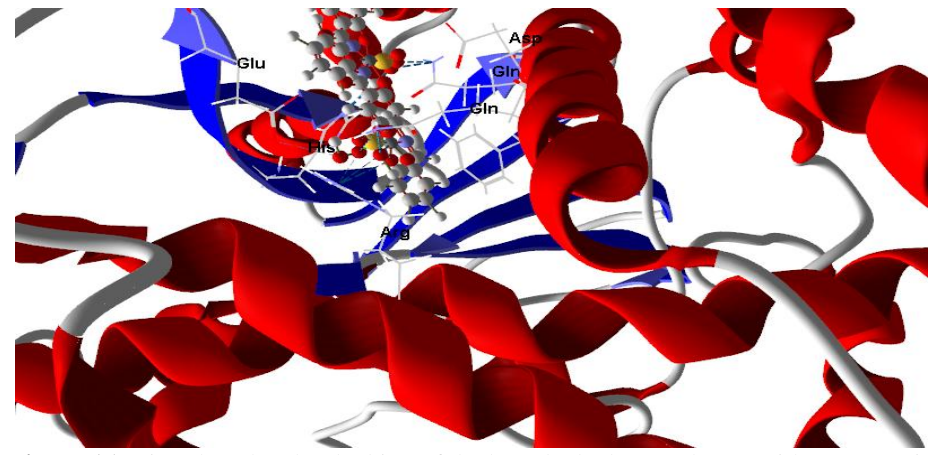


Figure (7) Virtual Molecular docking of the best docked (complex 3) with 3s7sprotein

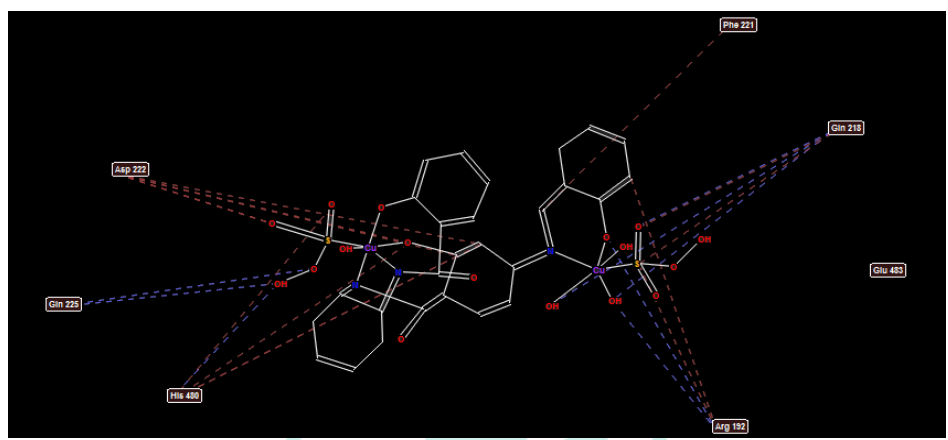


Figure (8) 2D structure of Molecular docking of (complex 3) with 3s7sprotein

Complex 4

However, the docked (complex 4) Fig. 9 have effective ligand-receptor interaction distances were \leq 3.5 A in most cases, which indicates the presence of typical real bonds and hence high binding affinity. For example, the nearest interaction is observed via H-donors with 3S7S (2,71A) and (complex 4) With Moldock score155188 Furthermore, eighteen binding sites were observed of different amino acids(Gln225, Glu483, His 480, Asp222, and Ile474) with complex 4

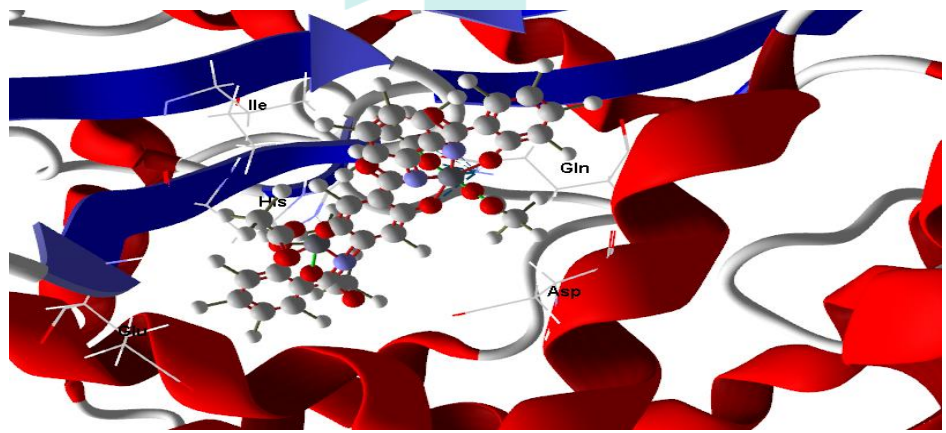


Figure (9) Virtual Molecular docking of the best docked (complex 4) with 3s7sprotein

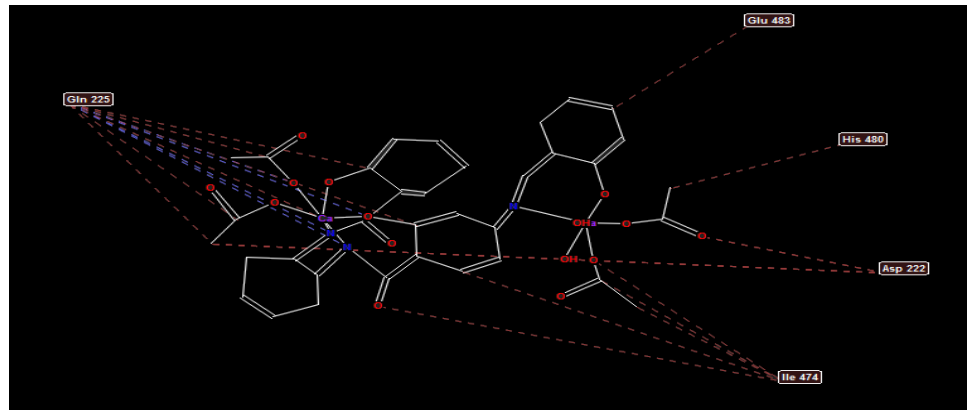


Figure (10) 2D structure of Molecular docking of (complex 4) with 3s7sprotein

Hence complex 2> complex 4> complex 3> complex 1> ligand towards inhibition of Brest cancer protein 3s7s.

Electron spin resonance (ESR)

The ESR spectral data for complexes (2),(4), and (7) are presented in Table (5). The spectra of copper(II) complexe (2) was characteristic of species, d⁹configuration having axial type of a $d(x^2-y^2)$ ground state which is the most common for copper(II) complexes [41,42]. The complexes show $g_{\parallel} > g_{\perp} > 2.0023$, indicating octahedral geometry around the copper (II) ion [43, 44]. The g-values are related by the expression $G = (g_{\parallel} - 2)/(g_{\perp} - 2)$ [45-47], where (G) is exchange coupling interaction parameter. If G < 4.0, a significant exchange coupling is present, whereas if G value > 4.0, local tetragonal axes are aligned parallel or only slightly misaligned.

Complex (2) show 2.24 value, indicating spin- exchange interactions take place between copper(II) ions. This phenomena is further confirmed by the magnetic moments values which were found in the (1.65–1.67 B.M.) range. The $g_{\parallel}/A_{\parallel}$ value is also considered as a diagnostic term for stereochemistry [48], the $g_{\parallel}/A_{\parallel}$ values were in the (153 cm⁻¹) range which are expected for distorted octahedral copper(II) complexes (Table 6). The g-value of the copper(II) complexes with a $2B_{1g}$ ground state ($g_{\parallel}>g_{\perp}$) may be expressed by [49]:

$$g_{\parallel} = 2.002 - (8K_{\parallel}^2 \lambda^{\circ}/\Delta Exy)$$
 (2)
 $g_{\perp} = 2.002 - (2K_{\perp}^2 \lambda^{\circ}/\Delta Exz)$ (3)

Where k_{\parallel} and k_{\perp} are the parallel and perpendicular components respectively of the orbital reduction factor (K), λ° is the spin-orbit coupling constant for the free copper, ΔExy and ΔExz are the electron transition energies of $2B_{1g} \rightarrow 2B_{2g}$ and $2B_{1g} \rightarrow 2E_{g}$. From the above relations, the orbital reduction factors $(K_{\parallel}, K_{\perp}, K)$, which are measure terms for covalency [50], can be calculated. For an ionic environment, K=1; while for a covalent environment, K<1. The lower the value of K, the greater is the covalency.

$$K^{2} = (g - 2.002) \Delta E /2\lambda (4)$$

$$K^{2} = (g - 2.002) \Delta E /8\lambda$$

$$K^{2} = (K^{2} + 2K2^{\perp})/3$$
(6)

K values Table (6), for the copper(II) complexe (2) was indicating covalent bond character [51, 54]. Kivelson and Neiman noted that, for ionic environment $g_{\parallel} \ge 2.3$ and for a covalent environment $g_{\parallel} < 2.3$. Theoretical work by Smith seems to confirm this view [55]. The g-values reported here Table 6 show considerable covalent bond character [50]. Also, the inplane σ -covalency parameter, $\alpha^2(Cu)$ was calculated by;

$$\alpha^{2}(Cu)=(A_{\parallel}/0.036)+(g_{\parallel}-2.002)+3/7(g_{\perp}-2.002)+0.04$$
 (7)

The calculated values (Table 6) suggest a covalent bonding [54, 55]. The in-plane and out of-plane π - bonding coefficients β_1^2 and β^2 respectively, are dependent upon the values of ΔExy and ΔExz in the following equations [55].

$$α2β2 = (g_{\perp}- 2.002) ΔExy/2λο$$
(8)
$$α2 β12 = (g|| - 2.002) ΔExz/8λο$$
(9)

In this work, the complexe (2) show β^2 value 0.89 indicating moderate degree of covalency in the in-plane π -bonding [53-55]. The value for complex (7) are 2.2 indicating ionic quaracter of the out-of-plane, It is possible to calculate approximate orbital populations ford orbitals [55] by:

$$A_{\parallel} = A_{iso} - 2B[1 \pm (7/4) \Delta g_{\parallel}] \Delta g_{\parallel} = g_{\parallel} - g_{e}$$
 (10)
 $a_{d}^{2} = 2B/2B^{\circ}$ (11)

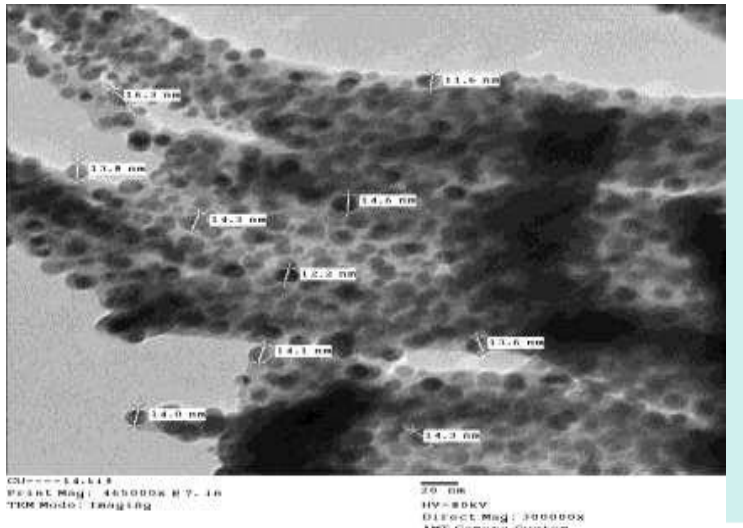
Where A° and $2B^{\circ}$ is the calculated dipolar coupling for unit occupancy of d orbital respectively. When the data are analyzed, the components of the [60] Cu hyperfine coupling were considered with all the sign combinations. The only physically meaningful results are found when A_{\square} and A_{\square} were negative. The resulting isotropic coupling constant was negative and the parallel component of the dipolar coupling 2B are negative (Table 5). These results can only occur for an orbital involving the dx^2-y^2 atomic orbital on copper. The value for 2B is quite normal for copper(II) complexes. The $|A_{iso}|$ value was relatively small. The 2B value divided by ${}^2B_{\circ}$ (The calculated dipolar coupling for unit occupancy of dx^2-y^2 (235.11 G), using equation (11) suggests all orbital population are 64.9, 52.5, 60 and 56.7 % d-orbital spin density, clearly the orbital of the unpaired electron is dx^2-y^2 . However, Co(II) complex (5) and Fe(III) complex (9) showed isotropic spectra with g_{iso} 2.007 and 2.01 with covalent bond character.

Complex	g	g⊥	gis a	A (G)	A⊥ (G)	A _{is} o	Gc	ΔE _{XY} (cm ⁻¹)	ΔE _{XZ} (cm ⁻¹)	K1 ²	K ₁ ²	к2	K	g /A (cm ⁻¹)	α ²	β ²	2 1β	-2β	a ² d(%)
2		2.06	2.12	140	5	50	4.0	17543	22831	0.79	0.63	0.74	0.87	153.4		1.1	0.89	152.5	64.9
4	2.25	2.05	2.117	145	10	55	5.0	18349	23809	0.69	0.69	0.69	0.83	150	0.73	0.94	0.94	140	60.0
5	-	-	2.007	-	-	-	-	-	-	-	-	-	-	-	-	-	-	-	-
7	2.20	2.05	2.10	120	7.5	45	4.0	17699	22472	0.65	0.53	0.61	0.78	179	0.6	1.08	0.88	123	52.5

 $g_{iso} = (g_{\parallel}-2)/(g_{\perp}-2), a=(g_{\parallel}+2g_{\perp})/3$

Transmission electron microscope characterization (TEM)

The average diameter of the two complexes particles Cu(II) and Zn(II) was determined to be 13.81 ± 1.447 nm and 23.975 ± 7.639 nm respectively. All complexes are present in nano size particles i.e., their particles present in a diameter between 1 and 100 nm in size.



20.5 mm

20.5 mm

20.5 mm

20.5 mm

20.5 mm

10.5 mm

Figure 3 TEM images for Cu(II) complexes nanoparticles

Figure 4 TEM images for Zn(II) complexes nanoparticles

All complexes are present in nano size particles i.e., their particles present in a diameter between 1 and 100 nm in size that exhibit new or enhanced size-dependent properties compared with larger particles of the same material with many advantages such as: Increased bioavailability, dose proportionality, decreased toxicity, smaller dosage form (i.e., smaller tablet), stable dosage forms of drugs which are either unstable or have unacceptably low bioavailability in non-nanoparticulate dosage forms, increased active agent surface area results in a faster dissolution of the active agent in an aqueous environment, such as the human body, faster dissolution generally equates with greater bioavailability, smaller drug doses, less toxicity and reduction in fed/fasted variability.

BIOLOGICAL STUDIES

In vitro cytotoxicity

The cytotoxic activity of the ligand (1) and some metal complexes (2), and (4) were evaluated against (MCF-7) human breast cancer cell, (MCF-7 cell line) within $0.1-100~\mu g/L$ concentration range as shown in figure (3). The IC₅₀ values were calculated for each compound and results are presented in Figure (4). As shown, most complexes displayed significantly cytotoxic activities compared to the standard drug. Cytotoxicity activity of the complexes may be attributed to the central metal atom which was explained by Tweedy's chelation theory [56, 57]. Zinc (II) complex (4) showed the highest cytotoxicity effect with IC₅₀ value of 3.01 μ M, followed by complex (3) with IC₅₀ value 33 μ M and then complex (5) with IC₅₀ value 34.7 μ M. It was observed that all complexes are more active than the free ligand. This indicated enhancing of the antitumor activity upon coordination. The enhancement of cytotoxic activity may be assigned to that the positive charge of the metal increased the acidity of coordinated ligand that bears protons, leading to stronger hydrogen bonds which enhanced the biological activity [58]. It seems that changing the anion, coordination sites, and the nature of the metal ion has a pronounced effect on the biological behavior by altering the binding ability of DNA [59]. Gaetke and

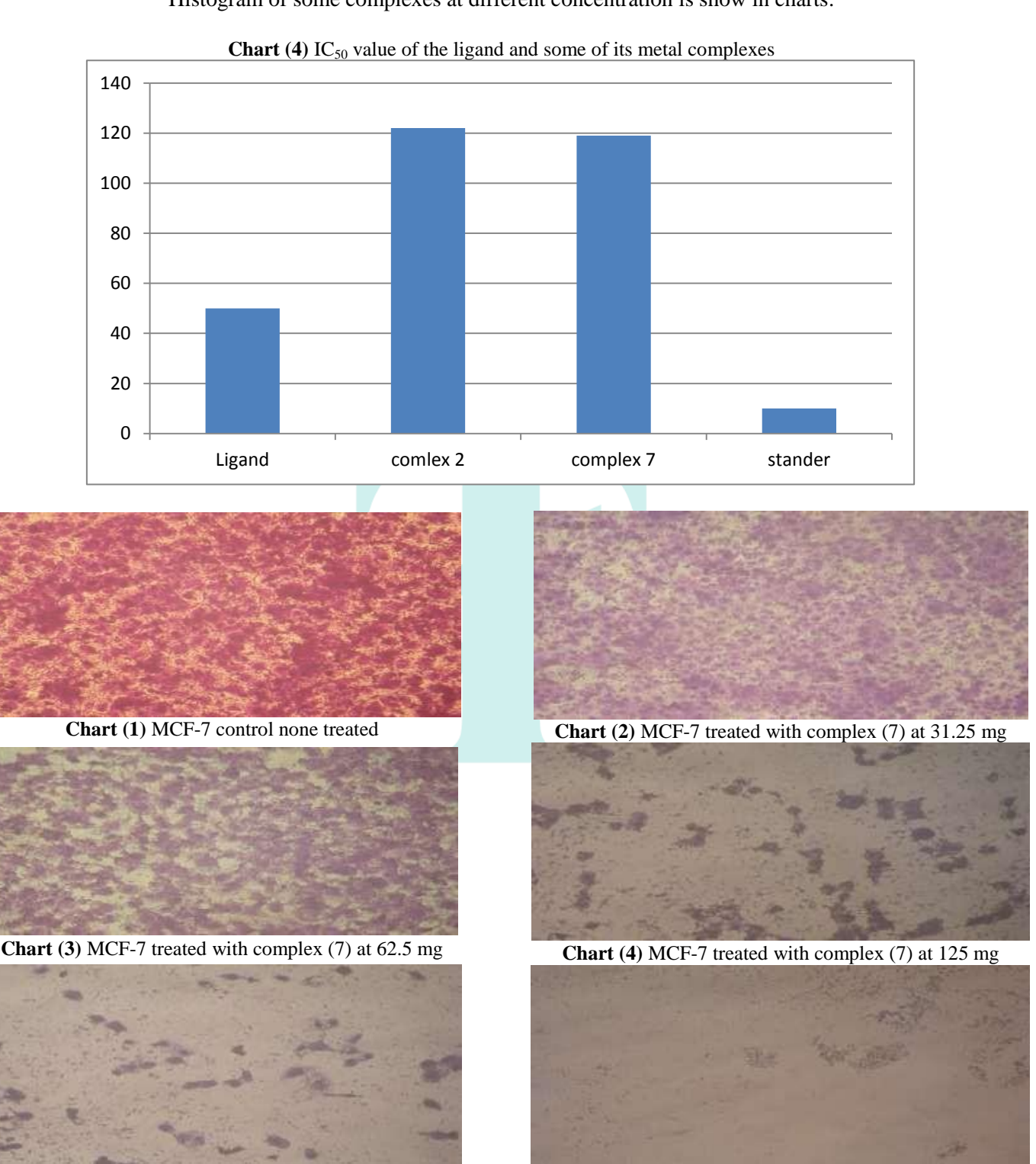
Chow had reported that metal has been suggested to facilitate oxidative tissue injury through a free radical mediated pathway analogous to the Fenton reaction [60].

By applying the ESR-trapping technique, evidence for metal - mediated hydroxyl radical formation in vivo has been obtained [55, 56]. Reactive oxygen species are produced through a Fenton-type reaction as follows:

$$LM(II) + H_2O_2 \rightarrow LM(I) + OOH + H^+ LM(I) + H_2O_2 \rightarrow LM(II) + OH + OH^-$$

where L, organic ligand

Histogram of some complexes at different concentration is show in charts:



CONCLUSION

Materials and Methods

Chart (5) MCF-7 treated with complex (7) at 250 mg

All reagents employed for the preparation of ligand and its metal complexes were of the analytical grade and used without further purification. Metal salts were provided from Sigma-Aldrich Company. Alanine amino acid (Assay \geq 99.99%), hydrazine hydrate (Assay \geq 98%), salicylaldhyde (Assay \geq 97%), H_2SO_4 (Assay 99.7%) and ethanol (Assay \geq 99.8%) were also obtained from Sigma-Aldrich Company.

Chart (6) MCF-7 treated with complex (7) at 500 mg

Physical and spectroscopic techniques

The characterization of the ligand and its corresponding metal complexes were carried out using various spectroscopic techniques.

Elemental analyses

Elemental analyses (C, H, N, Cl and M) for the ligand and its complexes were performed in Analytical Laboratory, Cairo University, Egypt.

Molar conductivity

The molar conductivity of 10⁻³ M of metal complexes in dimethyl sulfoxide (DMSO) was determined using Bibby conductimeter MCI at room temperature. The molar conductivities were calculated according to the Following equation:

$$\Lambda = VKMw/g\Omega$$

where $\Lambda = \text{Molar conductivity (ohm}^{-1}\text{cm}^2\text{ mol}^{-1})$

 $V = Volume \ of \ the \ solution \ (100 \ cm^3) \ K = Cell \ constant; \ 0.92 \ cm^{-1}$

Mw = Molecular weight of the complex

g = Weight of the complex dissolved in 100 cm³ solution

 Ω = Resistance measured in ohms

Mass spectra

The Mass spectra of the ligand and its metal complexes were recorded using JEUL JMS-500 mass spectrometer.

Thermal analyses

The thermal analyses (DTA and TGA) were carried out on a Shimadzu DT-50 thermal analyzer from room temperature to 800 °C at a heating rate of 10 °C/min.

¹H-NMR spectra

The ¹H-NMR spectra were record on Varian mercury VX-300 MHz NMR spectrometer in deuterateddimethylsulfoxide (DMSO-d₆) as a solvent. Chemical shifts (ppm) are reported relative to TMS.

IR spectra

FT- IR spectra of the ligand and its metal complexes were measured using KBr discs with Jasco FT/IR 6100 type A infrared spectrophotometer covering the range 400-4000 cm⁻¹.

Electronic absorption spectra

The electronic absorption spectra of the investigated compounds were recorded on Unico 4802 UV/Vis. double beam spectrophotometer (190-1100 nm). The electronic absorption spectra of both ligand and its metal complexes were recorded using ¹-cm quartz cells using DMSO as a solvent

Magnetic susceptibility

The magnetic susceptibilities of the complexes in the solid state were measured in a borosilicate tube with a Johnson Matthey. Magnetic Susceptibility Balance at room temperature using the following equations:

$$x_a = [2.068 \text{ L (R-R}^\circ) / (10^9 \text{W})]$$

 $x_m = x_a \times \text{MW}$
 $x_n = x_m - D$
 $\mu'_{eff} = 2.828 (x_n \times T)^{1/2}$

where x_a = Mass susceptibility

L = Sample length in cm

 $R = \text{Tube} + \text{sample reading } R^{\circ} = \text{Empty tube reading } W = \text{Mass of the sample } x_{\text{m}} = \text{Molar susceptibility } Mw = \text{Molar susceptibility$

Molecular weight

 x_n = Corrected molar susceptibility

D = Diamagnetic corrections

 μ_{eff} = Effective magnetic moment

T = Room temperature in Kelvin

The theoretical effective magnetic moment value calculated using the equation:

$$\mu_{\text{eff}} = [n (n+2)]^{1/2}$$

where

 μ_{efft} = Theoretical effective magnetic moment

n = the number of the unpaired electrons Diamagnetic corrections were made by interpretation of Pascal's constant [178].

ESR spectra

The solid ESR spectra of metal complexes were recorded with ELEXSYS E500 Bruker spectrometer in 3-mm Pyrex Tubes at 298°K. 2,2-Diphenyl-1-picrydrazide (DPPH), was used as a g-marker for the calibration of the spectra. The equation used to determine g-values is:

$$g = (g_{DppH}) (H_{DppH}) / H$$

where $g_{DppH} = 2.0036$

H _{DppH}= Magnetic field of DPPH in gauss

H = Magnetic field of the sample in gauss

FUNDING INFORMATION

This research did not receive any specific grant from funding agencies in the public, commercial, or not-for-profit sectors.

DECLARATION OF CONFLICT

The authors declare that they have no known competing financial interests or personal relationships that could have appeared to influence the work reported in this paper.

ACKNOWLEDGMENTS

The authors are grateful to interest.

REFERENCES

- 1. Dhanaraj, C.J. and Johnson, J. Quinoxaline based bio-active mixed ligand transition metal complexes: Synthesis, characterization, electrochemical, antimicrobial, DNA binding, cleavage, antioxidant and molecular docking studies. Journal of Photochemistry and Photobiology B: Biology, 2015. 151: p. 100-109.
- 2. El-Tabla, A.S. Abdelwahed, M. M and Whaba, M.A. Synthesis, characterization and fungicidal activity of binary and ternary metal(II) complexes derived from 4,4'-((4- nitro-1,2- phenylene)bis (azanylylidene))bis (3 -(hydroxyimino) hexan -2 one). Spectrochimica Acta Part A: Molecular and Biomolecular Spectroscopy, 2015. 136(Part C): p. 1941-1949.
- 3. Ajaykumar D Kulkarni .Schiff's Bases Metal Complexes in Biological Application. Journal of Analytical & Pharmaceutical Research 2017.V 5. Is1.
- 4. El-Tabla, A.S. Shakdofa, M.M.E and Whaba, M.A. Whaba, synthesis, characterization and antimicrobial activity of new Binary metal complexes derived from amino sulfonaphthalene ligand. Journal of Chemical, Biological and Physical Sciences, Section A, 2015. 5(4): p. 3629-3644.
- 5. El-Tabla, A.S. Abdelwahed, M. M. Organic amino acids chelates; preparation, spectroscopic characterization and applications as foliar fertilizers. Journal of Advances in Chemistry, 2014. 10(2): p. 2203-2217.
- 6. El-Tabla, A.S, Shakdofa. M.M.E and Whaba. M.A. Sugar hydrazone complexes; synthesis, spectroscopic characterization and antitumor activity. Journal of Advances in Chemistry, 2014. 9(1): p. 1837-1860.
- 7. El-Tabla, A.S., Abdelwahed, M. M and Whaba, M.A., Synthesis, characterization and fungicidal activity of binary and ternary metal(II) complexes derived from 4,4′- ((4-nitro -1,2-phenylene) bis (azanylylidene))bis(3-(hydroxyimino) hexan-2-one). Spectrochimica Acta Part A: Molecular and Biomolecular Spectroscopy, 2015. 136(Part C): p. 1941-1949.
- 8. Netalkar, P.P., S.P. Netalkar, and V.K. Revankar, Transition metal complexes of thiosemicarbazone: Synthesis, structures and invitro antimicrobial studies. Polyhedron, 2015. 100: p. 215-222.
- 9. El-Bahnasawy, R.M., {El-Bahnasawy, Ramadan M and El-Deen, Lobna M Sharaf and Abdou, S and Wahba, Mohammed A and El-Mensef, Abd I}electrical conductivity of salicylaldehyde thiosemicarbazone and Pd(II), Cu(II) AND Ru(III). Eur. Chem. Bull, 2014. 3(5): p. 441-446.
- 10. El-Bahnasawy, R.M., et al., Benzil bisisonicotinoyl hydrazone complexes of tervalent metals Ti, Zr, Sn, Hf and Th. J Inorg Biochem, 2013. 8((1)): p. 1-6.
- 11. Xia, L., Xia, Lei and Xia, Yu-Fen and Huang, Li-Rong and Xiao, Xiao and Lou, Hua-Yong and Liu, Tang-Jingjun and Pan, Wei-Dong and Luo, Heng}, Benzaldehyde Schiff bases regulation to the metabolism, hemolysis, and virulence genes expression in vitro and their structure–microbicidal activity relationship. European Journal of Medicinal Chemistry, 2015. 97: p. 83-93.
- 12. Chaitra, T.K., K.N.S. Mohana, and H.C. Tandon, Thermodynamic, electrochemical and quantum chemical evaluation of some triazole Schiff bases as mild steel corrosion inhibitors in acid media. Journal of Molecular Liquids, 2015. 211: p. 1026-1038.
- 13. Liang, J.-H., Liang, Jian-Hua and Lv, Wei and Li, Xiao-Li and An, Kun and Cushman, Mark and Wang, He and Xu, Ying-Chun}, Synthesis and antibacterial activity of oxime ether non-ketolides, and novel binding mode of alkylides with bacterial rRNA. Bioorganic & Medicinal Chemistry Letters, 2013. 23(5): p. 1387-1393.
- 14. El-Gamal, M.I., {El-Gamal, Mohammed I and Bayomi, Said M and El-Ashry, Saadia M and Said, Shehta A and Alaa, A-M and Abdel-Aziz, Naglaa I}, Synthesis and anti-inflammatory activity of novel (substituted) benzylidene acetone oxime ether derivatives: Molecular modeling study. European Journal of Medicinal Chemistry, 2010. 45(4): p. 1403-1414.
- 15. Dai, H., {Dai, Hong and Xiao, Yan-Shuang and Li, Zhong and Xu, Xiao-Yong and Qian, Xu-Hong}., The thiazoylmethoxy modification on pyrazole oximes: Synthesis and insecticidal biological evaluation beyond acaricidal activity. Chinese Chemical Letters, 2014. 25(7): p. 1014-1016.
- 16. Babahan, I., H. Anil, and N. Sarikavakli, Synthesis of vic-dioxime derivatives with hydrazone side groups and their metal complexes. Turkish Journal of Chemistry, 2006. 30(5): p. 563.

- 17. Ramanand R. Jeyamurugan "Synthesis, characterization, and DNA interaction of mononuclear copper(II) and zinc(II) complexes having a hard-"soft NS donor ligand." Journal of Coordination Chemistry, vol. 62, pp. 2375-2387, 2009.
- 18. El-Tabl, A.S., {El-Tabl, Abdou Saad and Mohamed Abd El-Waheed, Moshira and Wahba, Mohammed Ahmed and El-Fadl, Abd El-Halim Abou and others}, Synthesis, characterization and anticancer activity of new metal complexes derived from 2-hydrox y-3-(hydroxyimino)-4 -oxohexan -2-ylidene) benzohydrazide Journal of Advances in Chemistry, 9, 1837-1860 (2014).
- 19. Levander, O.A., Metabolic interrelationships between arsenic and selenium. Environmental Health Perspectives, 19: p. 159. 1977
- 20. Boyce, R., The Treatment of Sleeping Sickness and other Trypanosomiases by the Atoxyl and Mercury Method. British Medical Journal, 2(2437): p. 624. 1907
- 21. Lever and Philip, A. B. Inorganic electronic spectroscopy. Amsterdam: Elsevier, 1968. 22.
- 22. Bosch, F. and L. Rosich, *The contributions of Paul Ehrlich to pharmacology: a tribute on the occasion of the centenary of his Nobel Prize.* Pharmacology, 2008. 82(3): p. 171-179.
- 23. Shaikh Khaled, Mohammed Zamir Ahmed,Firdous G. Khan and Shaikh Kabeer Ahmed Synthesis, Characterization, and Photophysical Studies of Some Novel Ruthenium(II) Polypyridine Complexes Derived fromBenzothiazolylhydrazone. International Journal of Inorganic Chemistry, 2013. ID 212435, 7 pages
- 24. Vogel, A. ELBS, Vogel's textbook of quantitative inorganic analysis, including elementary instrumental analysis 4th. Edn. London and New York.
- 25. Naskar, S., {Naskar, Sumita and Naskar, Subhendu and Mondal, Satyajit and Majhi, Paresh Kumar and Drew, Mike GB and Chattopadhyay, Shyamal Kumar}, Synthesis and spectroscopic properties of cobalt (III) complexes of some aroyl hydrazones: X-ray crystal structures of one cobalt (III) complex and two aroyl hydrazone ligands. Inorganica Chimica Acta, 2011. 371(1): p. 100-106.
- 26. Bakheit and Satyanarayana.S, Vitamin B12 Model complexes: synthesis and characterization of thiocyanato cobaloximes and thiocyanato bridged dicobaloximes of o-donor ligands: DNA Binding and antimicrobial activity J. Korean Chem. Soc., 2010 6(54): p. 687.
- 27. El-Tabl, A.S. Synthesis and physico-chemical studies on cobalt (II), nickel (II) and copper (II) complexes of benzidine diacetyloxime. Transition Metal Chemistry, 2002. 27(2): p. 166-170.
- 28. Aly, M., Baghlaf. A and Ganji.N.Linkage isomerism of the oximato group: the characterization of some mono-and binuclear square planar nickel (II) complexes of vicinal oxime-imine ligands. Polyhedron, 1985. 4(7): p. 1301-1309.
- 29. Nakamoto, K. Infrared and Raman spectra of inorganic and coordination compounds. 1978: Wiley Online Library.
- 30. El-Tabl, A.S, Abdelwahed, M.M; Whaba, M. A.and Shebl, Synthesis, spectroscopic characterization and biological activity of the metal complexes of the Schiff base derived from phenylaminoacetohydrazide and dibenzoylmethane. Spectrochimica Acta Part A: Molecular and Biomolecular Spectroscopy, 2014. 71(1): p. 90-99.
- 31. El-Tabl, A.S.Novel N, N-diacetyloximo-1, 3-phenylenediamine copper (II) complexes. Transition Metal Chemistry, 1997. 22(4): p. 400-405.
- 32. Aly, M.M. and Imam,S.M. Site occupancy and reactivity of nickel (II) and palladium (II) coordination compounds of vicinal oxime-imine ligands: an interpretation to the phenomenon of chelate isomerism in the same molecule. Polyhedron, 1994. 13(12): p. 1907-1916.
- 33. El-Reash, G.M.A., K.M. Ibrahim, and Bekheit, M.M. Ligational behaviour of biacetylmonoxime nicotinoyl hydrazone (H2BMNH) towards transition metal ions. Transition Metal Chemistry, 1990. 15(2): p. 148-151.
- 34. Narendra Kumar Chaudhary and Parashuram Mishra. Metal Complexes of Novel Schiff Base Based on Penicillin: Characterization, Molecular Modeling, and Antibacterial Activity Study .Bioinorganic Chemistry and Applications. 2017, ID 6927675.
- 35. Lever, A., Electronic spectra of some transition metal complexes: Derivation of Dq and B. Journal of Chemical Education, 1968. 45(11): p. 711.
- 36. Aslan, H.G., Özcan, S. and Karacan, N. Synthesis, characterization and antimicrobial activity of salicylaldehyde benzenesulfonyl hydrazone (< i> Hsalbsmh and its Nickel (II), Palladium (II), Platinum (II), Copper (II), Cobalt (II) complexes. Inorganic Chemistry Communications, 2011. 14(9): p. 1550-1553.
- 37. Mohamed, G.G., Omar,M. and Hindy, A.M. Synthesis, characterization and biological activity of some transition metals with Schiff base derived from 2-thiophene carboxaldehyde and aminobenzoic acid. Spectrochimica Acta Part A: Molecular and Biomolecular Spectroscopy, 2005. 62(4): p. 1140-1150.
- 38. Geary, W.J., The use of conductivity measurements in organic solvents for the characterisation of coordination compounds. Coordination Chemistry Reviews, 1971. 7(1): p. 81-122.
- 39. El-Tabl, A.S., Abdelwahed, M. M.; Whaba, M. A Synthesis, spectroscopic investigation and biological activity of metal (II) complexes with N₂O₄ ligands. Journal of Chemical Research, 2009. 2009(9): p. 582-587.
- 40. Surati, K.R. and Thaker,B. Synthesis, spectral, crystallography and thermal investigations of novel Schiff base complexes of manganese (III) derived from heterocyclic β-diketone with aromatic and aliphatic diamine. Spectrochimica Acta Part A: Molecular and Biomolecular Spectroscopy, 2010. 75(1): p. 235-242.
- 41. Surati, K.R., Synthesis, spectroscopy and biological investigations of manganese (III) Schiff base complexes derived from heterocyclic β-diketone with various primary amine and 2, 2'-bipyridyl. Spectrochimica Acta Part A: Molecular and Biomolecular Spectroscopy, 2011. 79(1): p. 272-277.
- 42. Figgis, B.N., Introduction to Ligand Fields. 1966, Interscience Publishers.
- 43. Akbar Ali, M., Ali, Mohammad Akbar and Mirza, Aminul Huq and Yee, Chiam Yin and Rahgeni, Hayatti and Bernhardt, Paul V}, Mixed-ligand ternary complexes of potentially hexadentate but functionally tridentate Schiff base chelates. Polyhedron, 2011. 30(3): p. 542-548.
- 44. El-Tabl, A.S., Abdelwahed, M. M.; Whaba, M. A Synthesis of novel metal complexes with isonicotinoyl hydrazide and their antibacterial activity. Journal of Chemical Research, 2010. 34(2): p. 88-91.

- 45. Karlin, K.D. and Zubieta, J. Copper Coordination Chemistry: Biochemical & inorganic Perspectives. 1983: Adenine Press.
- 46. Hathaway, B. and Billing, D. The electronic properties and stereochemistry of mono-nuclear complexes of the copper (II) ion. Coordination Chemistry Reviews, 1970. 5(2): p. 143-207.
- 47. Al-Hakimi, A.N. El-Tabl, A.S. and Shakdofa, M.M. Coordination and biological behaviour of 2-(p-toluidin) -N'-(3-oxo-1,3-diphenyl propylidene) acetohydrazide and its metal complexes. Journal of Chemical Research, 2009. 2009(12).
- 48. Lakshmi Narayana Suvarapu, Young Kyo Seo, Sung Okbaek and Varada Reddy Ammireddy. Review on Analytical and Biological applications of Hydrazones and their Metal Complexes. Journal of Chemistry. 2012, 9(3), 1288-1304.
- 49. Smith, D., Chlorocuprates (II). Coordination Chemistry Reviews, 1976. 21(2): p. 93-158.
- 50. Kivelson, D. and R. Neiman, ESR studies on the bonding in copper complexes. The Journal of Chemical Physics, 1961. 35(1): p. 149-155.
- 51. Eltabl, A. S; Wahba, M. A. S. EL-assaly, A. L. Saad, M. Sugar Hydrazone Complexes; Synthesis, Spectroscopic Characterization and Antitumor Activity. Journal of Advances in Chemistry, 2014. 9(1): p. 1837-1860.
- 52. Surati, K. R. and Thaker, B. Spectrochimica Acta Part A: Molecular and Biomolecular Spectroscopy. 2010, 75, 235-242.
- 53. Mitu, L. Ilis, M. Raman, N.Imran, M. And Ravichandran. S.Transition Metal Complexes Isonicotinoyl –hydrazone -4-diphenylaminobenzaldehyde:Synthesis, Characterization and Antiumer Studies. E-Journal of Chemistry. 2012, 9(1), 365-372.
- 54. Z. Wail Al, "Synthesis of macrocyclic schiff bases based on pyridine-2, 6-dicarbohydrazide and their use in metal cations extraction," Organic Chemistry Current Research, 2012.
- 55. P. G. Avaji, S. A. Patil, and P. S. Badami, "Synthesis, spectral, thermal, solid-state DC electrical conductivity and biological studies of Co(II) complexes with Schiff bases derived from 3-substituted-4-amino-5-hydrazino-1, 2, 4-triazole and substituted salicylaldehydes," Transition Metal Chemistry, vol. 33, pp. 275-283, 2008.
- 56. V. Opletalová, D. S. Kalinowski, M. Vejsová, J. í. Kuneš, M. Pour, J. Jampílek, et al., "Identification and characterization of thiosemicarbazones with antifungal and antitumor effects: cellular iron chelation mediating cytotoxic activity," Chemical Research in Toxicology, vol. 21, pp. 1878-1889, 2008.
- 57. A. S. El-Tabl, M. M. Shakdofa, and A. El-Seidy, "Synthesis, Characterization and ESR Studies of New Copper(II) Complexes of Vicinal Oxime Ligands," Journal of the Korean Chemical Society, vol. 55, pp. 603-611, 2011.
- 58. L. M. Lima, F. S. Frattani, J. L. dos Santos, H. C. Castro, C. A. M. Fraga, R. B. Zingali, et al., "Synthesis and anti-platelet activity of novel arylsulfonate—acylhydrazone derivatives, designed as antithrombotic candidates," European Journal of Medicinal Chemistry, vol. 43, pp. 348-356, 2008.
- 59. P. V. Bernhardt, J. Mattsson, and D. R. Richardson, "Complexes of cytotoxic chelators from the dipyridyl ketone isonicotinoyl hydrazone analogues," Inorganic Chemistry, vol. [232] D. A. Green, W. E. Antholine, S. J. Wong, D. R. Richardson, and C. R. Chitambar, "Inhibition of Malignant Cell Growth by 311, a Novel Iron Chelator of the Pyridoxal Isonicotinoyl Hydrazone Class Effect on the R2 subunit of Ribonucleotide Reductase," Clinical Cancer Research, vol. 7, pp. 3574-3579, 2001.45, pp. 752-760, 2006.
- 60. G.-F.Qi, Z.-Y.Yang, and D.-D. Qin, "Synthesis, characterization and DNA-binding properties of the Cu(II) complex with 7-methoxychromone-3-carbaldehyde-benzoylhydrazone," Chemical and Pharmaceutical Bulletin, vol. 57, pp. 69-73, 2009.